JOURNAL OF VIROLOGY, Mar. 2007, p. 2656–2662 Vol. 81, No. 6
0022-538X/07/$08.00+0 doi:10.1128/JVI.02020-06

Enhancement of Hepatitis B Virus Replication by the Regulatory X Protein In Vitro and In Vivo▽

Victor V. Keasler, Amanda J. Hodgson, Charles R. Madden, and Betty L. Slagle*

Department of Molecular Virology and Microbiology, Baylor College of Medicine, Houston, Texas 77030-3411

Received 15 September 2006/Accepted 12 December 2006

The 3.2-kb hepatitis B virus (HBV) genome encodes a single regulatory protein termed HBx. While multiple functions have been identified for HBx in cell culture, its role in virus replication remains undefined. In the present study, we combined an HBV plasmid-based replication assay with the hydrodynamic tail vein injection model to investigate the function(s) of HBx in vivo. Using a greater-than-unit-length HBV plasmid DNA construct (payw1.2) and a similar construct with a stop codon at position 7 of the HBx open reading frame (payw1.2*7), we showed that HBV replication in transfected HepG2 cells was reduced 65% in the absence of HBx. These plasmids were next introduced into the livers of outbred ICR mice via hydrodynamic tail vein injection. At the peak of virus replication, at 4 days postinjection, intrahepatic markers of HBV replication were reduced 72% to 83% in mice injected with HBx-deficient payw1.2*7 compared to those measured in mice receiving wild-type payw1.2. A second plasmid encoding HBx was able to restore virus replication from payw1.2*7 to wild-type levels. Finally, viremia was monitored over the course of acute virus replication, and at 4 days postinjection, it was reduced by nearly 2 logs in the absence of HBx. These studies establish that the role for HBx in virus replication previously shown in transfected HepG2 cells is also apparent in the mouse liver within the context of acute hepatitis. Importantly, the function of HBx can now be studied in an in vivo setting that more closely approximates the cellular environment for HBV replication.

Hepatitis B virus (HBV) infection is a major health problem worldwide, with more than 350 million chronically infected individuals who are at risk for developing severe liver disease, including hepatocellular carcinoma (12). The 3.2-kb HBV genome encodes a single regulatory protein termed HBx, but progress towards understanding the role of HBx in virus replication has been hindered by the lack of either a cell culture system or a convenient small animal model. Although initial studies suggested that HBx was not required for virus replication in cell culture (2), experiments with the highly related woodchuck hepatitis virus (WHV) system indicate that the WHV X protein (WHx) is required for virus replication in vivo (23). Other studies have demonstrated that WHVs carrying mutant WHx grow with attenuated kinetics in vivo, depending on the particular mutation (17, 22).

While many functions have been ascribed to HBx (reviewed in reference 5), most studies have been performed in cell culture and under conditions in which HBx is not required for virus replication. Two recent advances provide new approaches to investigate a role for HBx in the context of virus replication in vivo. The first is a plasmid-based replication assay that utilizes a greater-than-unit-length HBV genome of the ayw subtype (payw1.2) (15) and an identical plasmid containing a stop codon affecting HBx amino acid position 7 (payw1.2*7) (10). These plasmids were used to demonstrate that capsid-associated viral DNA from the HBx-deficient payw1.2*7 plasmid (versus payw1.2) was reduced significantly in transfected human hepatoblastoma (HepG2) cells (10) and that HBx-deficient payw1.2*7 complemented with a second plasmid encoding HBx was able to restore virus replication to wild-type levels (3, 8, 19).

A second advance that provides a new tool for studying HBx function utilized a related greater-than-unit-length HBV genome plasmid injected via the mouse tail vein under hydrodynamic conditions to induce acute hepatitis (21). In this system, the HBV plasmid DNA directs the synthesis of authentic viral transcripts, leading to packaging of viral RNA and the release of virus particles into the blood. The effect of HBx deficiency on HBV replication in the hydrodynamic mouse model has not been examined. Therefore, the present study was designed to investigate a role for HBx in HBV replication in this in vivo model. We show that HBV replication in injected mice is both HBx dependent and HBx independent, with the former constituting approximately 75% of the virus replication observed in the liver and 99% of the viremia. Importantly, this study establishes a new in vivo model with which to study HBx function within the context of acute virus replication.

MATERIALS AND METHODS

Plasmids. A plasmid carrying a greater-than-unit-length (129%) HBV genome (payw1.2; subtype ayw) and the same plasmid with a stop codon for amino acid 7 of HBx (payw1.2*7) were previously described (10, 15) and were obtained from Robert Schneider. Plasmids pSI-X and pSI-green fluorescent protein (GFP) were created by inserting the gene for HBx (adw2 subtype) or GFP into the multiple cloning site of a plasmid containing the simian virus 40 enhancer/early promoter vector (pSI; Promega). A plasmid encoding a heat-stable, secretable form of alkaline phosphatase (pSI-SEAP) was constructed by inserting the simian virus 40 enhancer/early promoter from the pSI vector into the BglII and EcoRI sites of the promoterless pSEAP2-Basic plasmid (Clontech). The promoterless pSEAP2-Basic plasmid was also utilized as a negative control in animal experiments, and a pSI plasmid carrying the gene for neomycin resistance (pSI-neo) was used as a negative control plasmid for HepG2 transfection experiments. All plasmids were prepared and purified using an endotoxin-free plasmid Maxi kit (QIAGEN).

* Corresponding author. Mailing address: Department of Molecular Virology and Microbiology, Baylor College of Medicine, BCM-385 One Baylor Plaza, Houston, TX 77030. Phone: (713) 798-3006. Fax: (713) 798-5075. E-mail: bslagle@bcm.edu.

▽ Published ahead of print on 20 December 2006.

Cell culture and plasmid transfection. HepG2 cells were obtained from the ATCC and used at an early passage. Cells were plated at a density of approximately 5×10^5 cells per 60-mm plate and were transfected 24 h after being plated, using TransIT (Mirus Bio Corporation) according to the manufacturer's protocol. At 2 h posttransfection, 2×10^6 untransfected HepG2 cells were added to each plate to create a confluent monolayer. Cells were fed daily with Eagle's medium containing 10% serum and were harvested at 5 days posttransfection.

Hydrodynamic injection, sacrifice, and harvest of livers. Approval for all experiments involving animals was obtained from the Institutional Animal Care and Use Committee at Baylor College of Medicine. Outbred Crl:CD-1(ICR) mice (10 to 13 weeks of age) were injected via the tail vein with plasmid DNA (18 μg DNA per mouse) diluted in phosphate-buffered saline (PBS) to a volume equivalent to 8% of the total body weight of each animal. Each animal received 9 μg of HBV plasmid DNA (either payw1.2 or payw1.2*7), 5 μg pSI-SEAP (encoding secretable, heat-stable alkaline phosphatase), and 4 μg of either pSI-X or control plasmid. Negative control animals received 5 μg pSI-SEAP and 13 μg of promoterless pSEAP2-Basic plasmid DNA. Tail vein injection was completed in 8 to 11 seconds, and mice were then housed in a biohazard facility until sacrifice. At sacrifice, mice were anesthetized and bled, and their livers were processed as previously described (7). Alanine aminotransferase (ALT) levels were determined for serum samples by using a COBAS Integra 400 Plus high-throughput analyzer.

Retro-orbital bleeding of mice. Blood was collected from mice on days 0, 1, 4, 7, and 10 postinjection by retro-orbital bleeding to measure viremia in the circulation. For this procedure, mice were anesthetized using isoflurane, and approximately 50 μl of blood was collected in a nonheparinized microhematocrit capillary tube (Fisher Scientific).

Measurement of heat-stable alkaline phosphatase. For quantitation of heat-stable serum alkaline phosphatase (expressed from plasmid pSI-SEAP, included in all injections), 10 μl of serum was heated at 65°C for 30 min to inactivate endogenous phosphatases. The heat-inactivated serum was then diluted 1:25 in sterile saline, added to 450 μl of alkaline phosphatase yellow (pNPP) liquid substrate (Sigma), and mixed, and the optical density at 405 nm was recorded at 0, 10, 20, and 30 min to calculate relative alkaline phosphatase levels for normalization among groups of injected animals.

Histological and immunohistological analysis. Liver tissue was processed as previously described and stained with hematoxylin and eosin for histological analysis (7). Paraffin-embedded sections were also cut, and the tissue was incubated with rabbit anti-HBcAg (Dakocytomation) or rabbit anti-proliferating cell nuclear antigen (anti-PCNA) (FL-261; Santa Cruz Biotechnology), with diaminobenzidine used as a chromogen, according to the manufacturer's protocol.

Western blot detection of HBV core. Liver extracts were prepared by homogenizing 25 mg of liver in extraction buffer (50 mM Tris-HCl, 100 mM NaCl, 1 mM EDTA, 1% NP-40, and 1% aprotinin). Following centrifugation to remove cellular debris, the protein concentration was determined using a DC protein assay kit (Bio-Rad). A total of 125 μg protein from each liver was separated in a 12% polyacrylamide gel and transferred to a nitrocellulose membrane (30 min each at 100 mA, 200 mA, 300 mA, and 400 mA). Following transfer, the membrane was blocked with 5% nonfat dry milk in PBS for 1 h. The membrane was then cut in half, and each filter was incubated with either anti-HBcAg (1:1,000; Dako) or anti-tubulin (1:1,000; Sigma) (used as a loading control) in 0.01% PBS plus 0.1% Tween 20 for 1 h. Membranes were washed with PBS-Tween and incubated for 1 h with a secondary antibody (1:1,000) conjugated to horseradish peroxidase (Pierce). Antibody-bound HBV core (or tubulin) protein was then detected using a SuperSignal West Femto kit (Pierce).

IP/Western blot detection of HBx. Two 60-mm plates of transfected HepG2 cells were harvested on day 3 posttransfection and pooled for each immunoprecipitation (IP) reaction, as described previously (1). Detection of HBx from mouse liver tissue was performed as described previously (18), using 6 mg of liver extract per IP reaction. For the Western blot, bound anti-HBx primary antibody (1:1,000) was detected using a horseradish peroxidase-conjugated anti-rabbit secondary antibody and a SuperSignal West Femto detection kit (Pierce).

Purification of capsid-associated viral DNA. Capsid-associated DNA was extracted as described previously (13), with modifications. Equivalent amounts of HepG2 cells or liver tissues were homogenized in 1 ml of lysis buffer (50 mM Tris, pH 7.5, 0.5% NP-40, 1 mM EDTA, and 100 mM NaCl) and mixed gently at 4°C for 1 h. Next, 10 μl of 1 M $MgCl_2$ and 10 μl of DNase I (10 mg/ml) were added and incubated for 2 h at 37°C. Viral cores were then precipitated by adding 35 μl (0.5 M) of EDTA and 225 μl of 35% polyethylene glycol and incubating them at 4°C for at least 30 min, after which the cores were concentrated by centrifugation and the pellet was resuspended in 10 mM Tris, 100 mM NaCl, 1 mM EDTA, 1% sodium dodecyl sulfate (SDS), and 20 μl of proteinase K (25 mg/ml) and incubated overnight. Viral DNAs released from lysed cores were extracted with phenol and chloroform, precipitated with isopropanol, and resuspended in Tris-EDTA. For purification of cores from serum, 25 μl of serum was incubated for 12 to 16 h at 37°C with 10 mM Tris, pH 7.5, 5 mM $MgCl_2$, 3 mM $CaCl_2$, and 10 μl of DNase I (10 mg/ml) in a 1-ml total volume. Viral cores were precipitated by adding 35 μl of 0.5 M EDTA and 225 μl of 35% polyethylene glycol and were incubated for at least 1 h at 4°C. Cores were concentrated by centrifugation, and the pellet was resuspended in 10 mM Tris, 100 mM NaCl, 1 mM EDTA, 1% SDS, and 20 μl of proteinase K (25 mg/ml) (approximately 400-μl total volume) and incubated at 37°C overnight. Viral DNA was then extracted using a QIAamp DNA Blood Mini kit (QIAGEN) following the manufacturer's protocol.

Southern blot hybridization. Resuspended capsid-associated viral DNAs were separated in 1% agarose gels and transferred to a positively charged nylon membrane. Membranes were probed with a ^{32}P-labeled HBV DNA probe, and quantitation was performed by densitometer scanning.

Real-time PCR detection of HBV DNA. Real-time PCR was used to quantitate capsid-associated DNA, using TaqMan real-time PCR primers (5′-AGAAACA ACACATAGCGCCTCAT-3′ and 5′-TGCCCCATGCTGTAGATCTTG-3′) and probe (5′-TGTGGGTCACCATATTCTTGGG-3′) (Applied Biosystems). Cycling parameters, performed with an Applied Biosystems 7000 sequence detection system, were as follows: 1 cycle at 50°C for 2 min; 1 cycle at 95°C for 10 min; and 40 cycles at 95°C for 15 s and 60°C for 60 s. Plasmid payw1.2 was diluted over a range of 10^7 to 10^0 and used as a standard, and all samples were analyzed in duplicate.

Purification of viral RNA and analysis by Northern blotting. RNAs were extracted from liver tissue by using an RNAqueous-4 PCR kit (Ambion) according to the manufacturer's instructions. Briefly, flash-frozen liver tissue was homogenized, and the RNAs were extracted, washed, and treated with DNase I to remove contaminating DNA. RNA yield and quality were then assessed by measuring the UV absorbance at 260 nm and separating the RNAs in a 1% formaldehyde gel to visualize 28S and 18S rRNAs. For viral RNA detection, 3 μg of total RNA was run in a formaldehyde gel, transferred to a membrane, and blotted with a ^{32}P-labeled HBV DNA probe. Hybridization of the same blots with a ^{32}P-labeled β-actin probe provided the loading control.

Quantitation and statistics. Northern, Southern, and Western blots were exposed on Kodak BioMax MS film and quantitated by densitometry analysis (Molecular Dynamics) and ImageQuant5.2 software. Quantitation of PCNA-positive hepatocytes was performed on coded tissue sections by counting positive nuclei in five random high-power fields (each containing approximately 300 hepatocytes) from livers of two or three representative animals from each injection group. Statistical significance for all experiments was determined by using Student's *t* test or the Mann-Whitney rank sum test (SigmaStat software). Error bars are reported as standard errors of the means, and significance was assigned for P values of <0.05.

RESULTS

HBx is required for wild-type levels of HBV replication in HepG2 cells. To examine the contribution of HBx to virus replication, equivalent numbers of HepG2 cells were transfected with payw1.2 or payw1.2*7 and a plasmid encoding GFP to control for transfection efficiency. Cells were harvested at 5 days posttransfection, viral cores were isolated, and the DNA was extracted. Capsid-associated viral DNA was detected by hybridization with a ^{32}P-labeled full-length HBV DNA probe and quantitated by densitometry analysis. The level of capsid-associated viral DNA measured in cells transfected with HBx-deficient payw1.2*7 was reduced an average of 65% (range, 60 to 80% in three independent experiments) relative to that measured in cells transfected with wild-type payw1.2 (Fig. 1A, lanes 1 and 2). The reduced level of viral DNA was restored to wild-type levels by cotransfection of a plasmid encoding wild-type HBx (pSI-X) (Fig. 1A, lane 3). Southern blot hybridization results were confirmed by real-time PCR quantitation of capsid-associated DNA, using primers that reside outside both the terminally redundant portion of payw1.2 (and payw1.2*7) and the *X* gene used to complement payw1.2*7 replication (Fig. 1B). A sensitive IP/Western blot was used to demonstrate

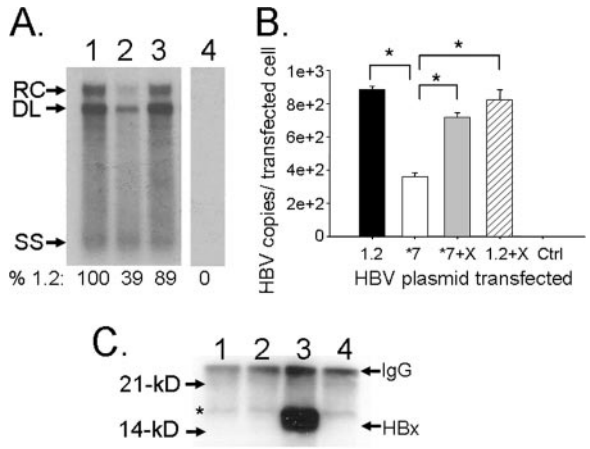

FIG. 1. HBx-dependent replication in transfected HepG2 cells. (A) Representative Southern blot detection of capsid-associated DNA. HepG2 cells transfected with payw1.2 (lane 1), payw1.2*7 (lane 2), payw1.2*7 plus pSI-X (lane 3), or the negative control plasmid pSI-neo (lane 4) were harvested, and capsid-associated DNAs were detected by agarose gel electrophoresis, electrophoretic transfer, and hybridization to a ^{32}P-labeled full-length HBV DNA probe. The different forms of viral DNA detected are identified at the left and include relaxed circular (RC), double-stranded linear (DL), and single-stranded (SS) forms. Filters were quantitated by densitometer scanning. The number at the bottom of each lane represents the relative level of HBV DNA, with that detected in cells transfected with payw1.2 set to 100% and that measured in cells receiving other HBV plasmids compared to the level with payw1.2. (B) Quantitation of capsid-associated viral DNA by real-time PCR. HBV capsid-associated DNAs purified from transfected HepG2 cells were diluted and analyzed by real-time PCR. Data are reported as the averages for three experiments ± standard errors of the means (SEM), and statistical significance is indicated by asterisks above the brackets. (C) Representative IP/Western blot. Cells transfected with payw1.2 (lane 1), payw1.2*7 (lane 2), payw1.2*7 plus pSI-X (lane 3), or the pSI-neo negative control (lane 4) were extracted and analyzed by IP/Western blotting for HBx. The migration of molecular size markers is shown at the left, and the locations of IgG bands and HBx are shown by arrows at the right. The asterisk identifies a nonspecific band detected in all lanes.

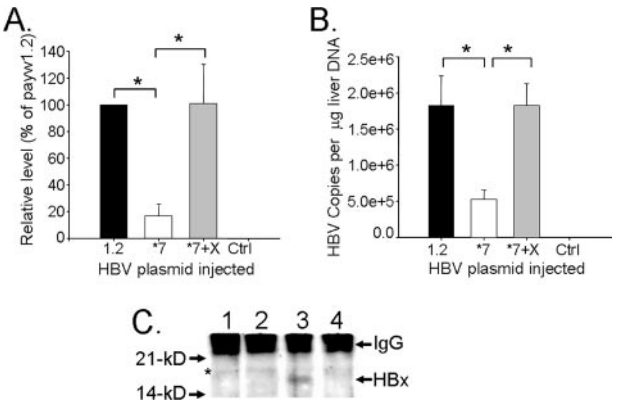

FIG. 2. HBx-dependent replication in the livers of hydrodynamically injected mice. (A) Quantitation of capsid-associated DNA by Southern blot hybridization and densitometer scanning. The amount of capsid-associated HBV DNA measured in mice injected with payw1.2 was set to 100%, and the relative levels of viral DNA detected in the livers of mice injected with other plasmids (payw1.2*7, payw1.2*7 plus pSI-X, or a control plasmid) are reported as percentages of that level. Five mice from each group were analyzed, and error bars (SEM) were derived per injection group. Statistical significance is denoted by asterisks above the brackets. (B) Quantitation of capsid-associated viral DNA by real-time PCR. Capsid-associated HBV DNAs were purified from liver tissue and quantitated by real-time PCR as described in Materials and Methods. Results shown are the averages for five mice per group ± SEM, and statistical significance is indicated by asterisks above the brackets. (C) Representative IP/Western blot detection of HBx. Liver extracts analyzed were from animals receiving payw1.2 (lane 1), payw1.2*7 (lane 2), payw1.2*7 plus pSI-X (lane 3), or control plasmid (lane 4). The arrows at the left indicate the migration of molecular size markers, and those at the right note the migration of IgG and HBx. The asterisk marks a nonspecific band migrating slightly above the 17-kDa HBx protein.

HBx expression in cells cotransfected with the complementing pSI-X plasmid DNA (Fig. 1C, lane 3). The expression of HBx from the payw1.2 template was below the limit of detection by our IP/Western assay (Fig. 1C, lane 1). In control experiments, we found that our rabbit anti-HBx antibody reacted 10-fold more strongly by IP/Western blotting to subtype adw2 HBx than to subtype ayw HBx, although both proteins showed an equivalent ability to transactivate a reporter construct (data not shown). Importantly, cotransfection of pSI-X with the wild-type payw1.2 plasmid did not lead to a further enhancement of HBV replication compared to that with payw1.2 alone, indicating that the level of HBx expressed from the payw1.2 template is sufficient for maximal HBV replication in this system (Fig. 1B). Together, these results are consistent with previous studies utilizing the same payw1.2 and payw1.2*7 plasmids (3, 8, 19) and demonstrate a requirement for HBx to obtain wild-type levels of HBV replication in HepG2 cells.

HBx is required for wild-type levels of capsid-associated HBV DNA in vivo. To extend these observations to an in vivo setting, the same plasmid DNAs were introduced into groups of five ICR mice by hydrodynamic tail vein injection (9). Outbred mice were used to avoid the possibility that our observations might be restricted to a specific inbred line of mice. A reporter plasmid DNA encoding a secretable form of heat-stable alkaline phosphatase was included with each injection to control for injection efficiency. Mice were sacrificed on day 4 postinjection, and viral capsids were purified from equivalent amounts of liver tissue. Capsid-associated DNA was analyzed by gel electrophoresis, hybridized to a radiolabeled HBV DNA probe, and scanned for densitometer quantitation. The level of capsid-associated DNA in the livers of mice receiving payw1.2*7 was reduced 83%, on average, relative to that measured in the livers of mice receiving payw1.2 (Fig. 2A). This was restored to wild-type (payw1.2) levels when a second plasmid encoding HBx (pSI-X) was used as a complement. The densitometer results (Fig. 2A) were confirmed by real-time PCR quantitation of purified capsid-associated DNA (Fig. 2B). The expression of HBx in the livers of injected mice was confirmed by IP/Western blotting for mice receiving the pSI-X plasmid to complement payw1.2*7 (Fig. 2C, lane 3), but the expression of HBx from the payw1.2 template was below the limits of detection with this assay (Fig. 2C, lane 1). These results demonstrate that the requirement of HBx for wild-type levels of capsid-associated viral DNA previously observed in HepG2 cells is also apparent in mouse hepatocytes in vivo. In addition, we concluded that in this model, approximately 75% of the virus replication observed is HBx dependent, while 25% of it occurs independent of HBx expression and is considered

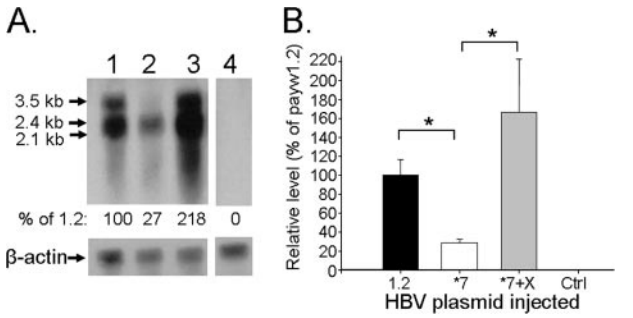

FIG. 3. Enhancement of HBV RNA by HBx in vivo. (A) Representative Northern blot for mice injected with payw1.2 (lane 1), payw1.2*7 (lane 2), payw1.2*7 plus pSI-X (lane 3), or a negative control plasmid (lane 4). Viral RNAs were detected by hybridization to a ^{32}P-labeled HBV DNA probe, quantitated by densitometer scanning, and normalized to a β-actin loading control. The detection of the three HBV RNA species (3.5, 2.4, and 2.1 kb) is shown by arrows at the left. (B) Densitometer quantitation of Northern blots. Following normalization of hybridization signals to loading controls, the level of viral RNA detected in mice injected with payw1.2 was set to 100%, and the level of viral RNA detected in mice injected with payw1.2*7, payw1.2*7 plus pSI-X, or a control plasmid is reported as a percentage of that detected in livers of mice receiving payw1.2. All data are reported as the averages for four or five mice per group ± SEM, and statistical significance is indicated by asterisks above the brackets.

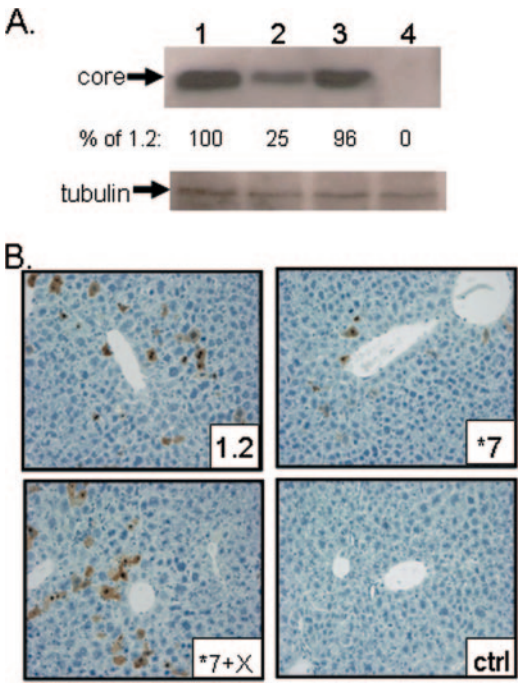

FIG. 4. Enhancement of HBV core protein level by HBx in vivo. (A) Representative HBV core Western blot. Liver tissue was detergent extracted from mice injected with payw1.2 (lane 1), payw1.2*7 (lane 2), payw1.2*7 plus pSI-X (lane 3), or a negative control plasmid (lane 4). Solubilized proteins were separated by SDS-polyacrylamide gel electrophoresis. Following transfer to a nitrocellulose filter, the HBV core protein was detected as described in Materials and Methods and quantitated by densitometer scanning and normalization to the signal obtained from a tubulin loading control. The level of core protein detected in mice receiving payw1.2 was set to 100% (lane 1), and levels in other mice (lane 2, payw1.2*7; lane 3, payw1.2*7 plus pSI-X; lane 4, negative control) were compared to that. (B) Detection of HBV core protein in paraffin-embedded liver tissue. Sections of liver tissue were incubated with rabbit anti-core, as described in Materials and Methods. Hepatocytes staining brown are positive for the core protein. Magnification, ×200.

to be residual replication (see Discussion). While the ability of HBx to enhance virus replication in vivo was previously demonstrated by crossing HBV transgenic mice lacking HBx with transgenic mice expressing HBx (20), that model lacked a host immune response to HBV proteins. The present study is the first report of a role for HBx in HBV replication within the context of acute hepatitis in vivo.

HBV RNAs and core protein are reduced in the absence of the HBx protein. To identify the step(s) in virus replication affected by HBx, liver tissues from mice sacrificed on day 4 postinjection were analyzed. Total liver RNA was extracted and analyzed by Northern blot hybridization using a radiolabeled HBV-specific probe. All three species of viral RNA (3.5, 2.4, and 2.1 kb) were detected in the livers of all mice receiving HBV plasmid DNA (Fig. 3A). When normalized to a β-actin loading control, there was an average 72% reduction in total HBV transcripts in the mice receiving payw1.2*7 relative to those in mice receiving payw1.2 (Fig. 3A, lanes 1 and 2, and B). These reduced levels were restored to greater-than-wild-type levels when mice injected with payw1.2*7 received a second plasmid encoding HBx (pSI-X) (Fig. 3A, lane 3, and B). These results suggest that one function of HBx in the HBV hydrodynamic model is to enhance the level of HBV mRNAs.

HBV core protein was similarly reduced in mice receiving HBx-deficient payw1.2*7 relative to that found in mice receiving payw1.2. The HBV core protein was detected by Western blotting using a rabbit anti-core antibody (Dakocytomation), and the signal was normalized by using tubulin as a loading control. Total HBV core protein was decreased 75% in mice injected with payw1.2*7 (Fig. 4A, lane 2) compared to that in mice injected with payw1.2 or payw1.2*7 plus pSI-X (Fig. 4A, lanes 1 and 3). Paraffin-embedded liver tissue was stained with an antibody to core protein to identify the pattern of infected hepatocytes within the liver. Approximately 5 to 7% of hepatocytes from mice injected with payw1.2 were strongly positive for HBV core protein (Fig. 4B). In contrast, staining of liver tissues from mice injected with payw1.2*7 yielded a noticeable decrease in the intensity of staining (Fig. 4B), and this was restored to wild-type levels for mice receiving both payw1.2*7 and a second plasmid encoding HBx (pSI-X). The core-positive hepatocytes were distributed evenly throughout the liver and were not restricted to specific zones (data not shown).

HBx enhances the level of circulating HBV. We next examined the effect of HBx on viremia during the course of acute hepatitis. Groups of mice received either payw1.2, payw1.2*7, payw1.2*7 plus pSI-X, or a negative control plasmid. Serum was collected by retro-orbital bleeding at 0, 1, 4, 7, and 10 days postinjection, and capsid-associated viral DNA was extracted and quantitated by real-time PCR. Viremia was maximal at day 4 postinjection, which is consistent with the result reported for a similar greater-than-unit-length HBV plasmid injected into B10.D2 mice (21). Very low levels of capsid-associated viral DNA were detected at day 1 postinjection in all groups of mice receiving HBV plasmid DNA (Fig. 5). Virus titers measured in mice injected with payw1.2*7 were significantly reduced com-

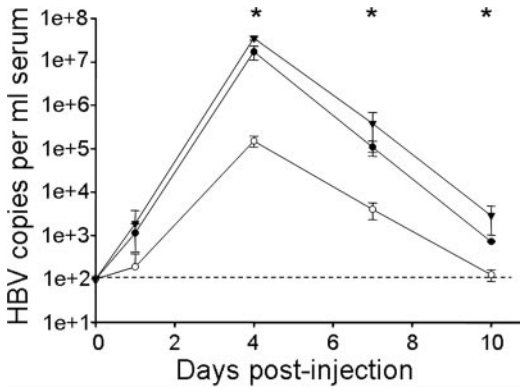

FIG. 5. Effect of HBx on circulating HBV. Mice were injected with payw1.2 (filled circles; $n = 7$ mice), payw1.2*7 (empty circles; $n = 10$ mice), or payw1.2*7 plus pSI-X (filled triangles; $n = 3$ mice), and blood was collected via the retro-orbital route on days 0, 1, 4, 7, and 10 postinjection. Capsid-associated HBV DNA was purified from serum and quantitated by real-time PCR. The dashed line represents the background copies of HBV DNA from the real-time PCR (0.2 copy per μl serum). Error bars represent SEM, and statistical significance (for payw1.2 versus payw1.2*7) is designated with asterisks.

pared to those in mice receiving payw1.2 at days 4, 7, and 10 postinjection (Fig. 5). The most dramatic reduction was measured at day 4 postinjection, when viremia in the payw1.2*7-treated animals was reduced 99% compared to that measured in mice receiving payw1.2 ($P < 0.05$). The results of two additional independent experiments revealed similar 97% and 98% reductions in viremia in the payw1.2*7 mice (data not shown). By day 10, the majority of the virus had been cleared from the sera of all injected mice. Following hydrodynamic injection, ALT levels were elevated in all groups on day 1 and had returned to baseline by day 4, with no significant differences measured between injection groups at any of the time points measured (days 0, 1, 4, and 7) (data not shown). The increased ALT levels on day 1 indicated injury to the livers of injected mice. We next performed staining for PCNA on livers of mice at 4 days postinjection to determine whether the liver injury led to compensatory regeneration. Livers of injected mice showed up to 15-fold increases in PCNA-positive staining relative to that measured in uninjected control mice (Table 1). There were no significant differences in PCNA positivity among groups of animals receiving different plasmids, including a control plasmid that did not encode HBV.

DISCUSSION

HBx is a conserved viral protein that is presumed by analogy to WHx (23) to be required for HBV replication in vivo. However, the lack of a suitable small animal model has hindered the identification of HBx functions that contribute to virus replication. The current study combined the greater-than-genome-length HBV plasmid DNA replication model (10) with the hydrodynamic model of acute hepatitis (21) to examine HBx function within the context of acute viral hepatitis. We show that in this model, 75% of the HBV capsid-associated DNA in the liver is dependent on HBx. An even more dramatic effect of HBx was measured at the level of viremia, where virus replication from the payw1.2*7 template was reduced up to 99% relative to that from the wild-type payw1.2 template. In all instances, the lower replication level from the payw1.2*7 plasmid was restored to wild-type levels by complementation with a second plasmid DNA encoding HBx. Together, these results demonstrate that the role for HBx in HBV replication previously described for human HepG2 cells is also evident in mouse hepatocytes in vivo. To our knowledge, this is the first report of a role for HBx in virus replication within the context of acute hepatitis in a small animal model.

There are several possible steps at which HBx may contribute to HBV replication in this animal model. The livers of mice receiving plasmid payw1.2*7 revealed a 72% reduction in viral transcripts compared to the levels measured in mice receiving wild-type payw1.2 (or payw1.2*7 plus pSI-X). This effect of HBx is consistent with the degree of HBx transactivation previously reported for a variety of cellular and viral promoters in cell culture (14) and would argue that the magnitudes of HBx transactivation are similar both in vivo and in immortalized cells in culture. Our finding that HBx enhances the level of HBV mRNA is in agreement with similar results from previous studies with HepG2 cells (8, 19) but differs from another report indicating that HBV mRNA levels in HepG2 cells are unaffected by HBx (3). While the reason for the latter discrepancy is unclear, note that our finding of reduced mRNA from the payw1.2*7 template is supported by the additional observation of reduced viral core protein levels. Therefore, we consider that the reduced mRNA measured in the absence of HBx may be sufficient to explain the reductions in the later steps in virus replication, including intrahepatic core protein and capsid-associated DNA. We conclude that one function of HBx in the hydrodynamic model is to increase the level of HBV mRNA.

While HBx deficiency yielded a marked effect on core-associated DNA within the liver, the effect of HBx was even more dramatic on the level of viremia. While the absence of HBx led to an approximately 75% reduction in intrahepatic viral mRNA, core protein, and capsid-associated DNA, the analysis of sera collected at the peak of virus replication, at day 4 postinjection, revealed a 99% reduction in viral titer in mice injected with payw1.2*7 (versus payw1.2) (Fig. 5; Table 2). This impressive reduction in viremia in the absence of HBx, compared to the relatively more modest reduction of intrahepatic viral markers, was unexpected. However, it has been shown that the core protein requires a critical concentration for dimerization and capsid formation (16), and thus it is possible that the decrease in viral mRNA and core protein in the

TABLE 1. Increased PCNA-positive hepatocytes in hydrodynamically injected mice

Plasmid(s) injected[a]	No. of mice (and livers) examined	% PCNA-positive hepatocytes[b]
payw1.2	3	2.07 ± 0.47*
payw1.2*7	3	4.38 ± 1.19*
payw1.2*7 plus pSI-X	3	3.47 ± 0.99*
Negative control plasmid	2	2.90 ± 0.72*
Uninjected control	3	0.29 ± 0.12

[a] Plasmid DNA was injected as described in Materials and Methods.
[b] Percentage of total hepatocytes staining positive for PCNA (by immunohistochemistry), reported as means ± SEM. Asterisks indicate statistically significant differences (by Student's t test) compared to uninjected animals ($P < 0.05$).

TABLE 2. Effects of HBx deficiency on levels of HBV capsid-associated DNA

Source of HBV	% Wild-type HBV DNA[a]	HBx subtype used to complement[b]	Reference
HepG2	5[c]	ayw (0)	3
	5[c]	ayw (0)	8
	25[c]	adr4 (7.8)	19
	35[c,d]	adw2 (5.8)	Present study
Mouse liver	25[c,d]	adw2 (5.8)	Present study
Mouse serum	1[c,d]	adw2 (5.8)	Present study

[a] Determined as follows: (capsid-associated DNA from HBx-deficient payw1.2*7/capsid-associated DNA from wild-type payw1.2) × 100.
[b] Numbers in parentheses indicate percent amino acid differences of a given HBx compared to the ayw subtype found in payw1.2.
[c] Quantitation by Southern blot hybridization and densitometry scanning.
[d] Quantitation by real-time quantitative PCR.

absence of HBx leads to an even stronger reduction in the level of assembled viral capsids. We also considered that a function of HBx may be needed for optimal capsid stability. There is an unconfirmed report of HBx "reactivity" in viral cores (4). However, HBx could indirectly affect capsid stability. For example, HBx enhances the phosphorylation of the HBV core protein at serine 162 and serine 170 (11), and it has been proposed that phosphorylation of the core at serine 87 affects the stability of HBV capsids, although the effect of HBx in that process was not examined (6). The phosphorylation status of the core protein was not studied in the injected mice. Other possibilities to explain the additional effect of HBx on viremia include an as yet undefined role for HBx in viral egress from the cell.

It is not clear why a previous study with woodchucks showed a complete failure of WHx-deficient WHV to grow in vivo (23) while the present study shows residual HBV replication in the absence of HBx. In the hydrodynamically injected mouse, the residual HBx-independent HBV replication comprises 25% of the total intrahepatic replication and 1% of the viremia. Similarities between these two models include the use of a greater-than-unit-length WHV (or HBV) plasmid DNA capable of expressing the 3.5-kb pregenomic RNA. Both models also utilized plasmid DNAs with an engineered stop codon designed to prevent WHx (or HBx) expression. However, there are also important differences in these two models that may explain the residual HBx-independent replication observed in hydrodynamically injected mice. It has been demonstrated that HBx is not required for HBV replication in dividing cells (2), and so the compensatory regeneration observed in response to hydrodynamic injection (Table 1) may provide a cellular environment that favors HBV replication even in the absence of HBx. This would be expected to occur in all groups of injected mice, since we did not observe differences in ALT levels or in the frequency of PCNA-positive hepatocytes among groups of mice receiving different plasmid DNAs. We also consider it possible that the efficient delivery of plasmid DNA by the hydrodynamic method (estimated in another study to reach 40% of hepatocytes, as measured with a sensitive beta-galactosidase assay [9]) may contribute to a higher "background" of residual HBx-independent replication in the mouse model. In summary, it is likely that a combination of the above differences in experimental systems could explain the apparently discrepant results for the effect of HBx deficiency on virus replication in these two models.

The host immune response to HBV replication in the hydrodynamic model was described previously (21). In that study, the decline of viremia was accompanied by both the appearance of antibodies to HBV core, surface, and e antigens and the development of HBV-specific cytotoxic T lymphocytes detectable in the spleens of mice by day 7. The successful host immune response led to disappearance of the virus from the blood by day 10 postinjection. While the experimental design of the present study did not specifically address the host immune response, note that the kinetics of virus clearance appeared to be similar for all mice receiving HBV plasmids (payw1.2, payw1.2*7, or payw1.2*7 plus pSI-X), indicating no obvious effect of HBx on the ability of the host immune response to clear replicating HBV in this model.

This is the first report of in vivo HBx complementation of payw1.2*7 HBx-deficient replication. However, previous studies have identified this property of HBx in plasmid-transfected HepG2 cells (Table 2). In those studies, the HBx subtypes ayw and adr were shown to complement HBx-deficient replication, whereas the present study examined the adw2 subtype. The HBx protein sequences deduced from cloned HBV isolates vary by up to 10% at the amino acid level, and those tested thus far in the complementation assay differ from each other by up to 7.8% at the amino acid level, yet all were able to similarly rescue HBV replication to wild-type (payw1.2) levels in HepG2 cells. Thus, certain amino acid positions within HBx can be varied without affecting the protein's ability to restore HBx-deficient replication to wild-type levels.

In the course of our study, we noted that the effect of HBx deficiency on HBV replication in HepG2 cells was apparent only under certain culture conditions (see Materials and Methods). Specifically, an effect of HBx deficiency on virus replication was noted when the HepG2 cells were confluent but not when the cells were growing and subconfluent. This observation was also reported by Leupin et al., using the same payw1.2 and payw1.2*7 plasmids (8). It was previously suggested that HBx may function to push cells out of quiescence, presumably to generate a cellular environment that favors virus replication (5). Regardless of the mechanism involved, these results provide an explanation for earlier studies in which it was concluded that HBx was not required for virus replication in cell culture (2).

In summary, we have used the hydrodynamic mouse model of acute hepatitis to examine a role for HBx in virus replication. We demonstrated that the requirement for HBx in virus replication previously described for transfected HepG2 cells is also apparent in mouse hepatocytes in vivo. In this model, the effect of HBx deficiency results in a consistent 75% reduction in viral mRNA, core protein, and capsid-associated viral DNA in the liver and a 99% reduction in circulating viremia. In all instances, the effects of HBx deficiency were reversed by adding a complementing plasmid encoding HBx. Importantly, this in vivo model permits further investigation into HBx's contributions to virus replication by the testing of mutant HBx proteins in a biologically relevant setting.

ACKNOWLEDGMENTS

Support for core facilities used in this research was provided through the Texas Gulf Coast Digestive Diseases Center (National Institutes of Health [NIH] grant DK56338). This work was also supported by NIH grant CA95388 (B.L.S.) and by an American Gastroenterology Association Foundation for Digestive Health and Nutrition Research scholar award (C.R.M.).

REFERENCES

1. **Becker, S. A., T. H. Lee, J. S. Butel, and B. L. Slagle.** 1998. Hepatitis B virus X protein interferes with cellular DNA repair. J. Virol. **72:**266–272.
2. **Blum, H. E., Z. S. Zhang, E. Galun, F. von Weizsäcker, B. Garner, T. J. Liang, and J. R. Wands.** 1992. Hepatitis B virus X protein is not central to the viral life cycle in vitro. J. Virol. **66:**1223–1227.
3. **Bouchard, M. J., L.-H. Wang, and R. J. Schneider.** 2002. Calcium signaling by HBx protein in hepatitis B virus DNA replication. Science **294:**2376–2378.
4. **Feitelson, M. A., M. M. Clayton, and B. Phimister.** 1990. Monoclonal antibodies raised to purified woodchuck hepatitis virus core antigen particles demonstrate X antigen reactivity. Virology **177:**357–366.
5. **Ganem, D., and R. J. Schneider.** 2001. *Hepadnaviridae*: the viruses and their replication, p. 2923–2969. *In* D. M. Knipe, P. M. Howley, D. E. Griffin, R. A. Lamb, M. A. Martin, B. Roizman, and S. E. Straus (ed.), Fields virology. Lippincott Williams & Wilkins, Philadelphia, PA.
6. **Kang, H. Y., S. Lee, S. G. Park, J. Yu, Y. Kim, and G. Jung.** 2006. Phosphorylation of hepatitis B virus core protein at Ser87 facilitates core assembly. Biochem. J. **398:**311–317.
7. **Keasler, V. V., H. Lerat, C. R. Madden, M. J. Finegold, M. J. McGarvey, E. M. A. Mohammed, S. J. Forbes, S. M. Lemon, D. L. Hadsell, S. J. Grona, F. B. Hollinger, and B. L. Slagle.** 2006. Increased liver pathology in hepatitis C virus transgenic mice expressing the hepatitis B virus X protein. Virology **347:**466–475.
8. **Leupin, O., S. Bontron, C. Schaeffer, and M. Strubin.** 2005. Hepatitis B virus X protein stimulates viral genome replication via a DDB1-dependent pathway distinct from that leading to cell death. J. Virol. **79:**4238–4245.
9. **Liu, F., Y. K. Song, and D. Liu.** 1999. Hydrodynamics-based transfection in animals by systemic administration of plasmid DNA. Gene Ther. **6:**1258–1266.
10. **Melegari, M., P. P. Scaglioni, and J. R. Wands.** 1998. Cloning and characterization of a novel hepatitis B virus X binding protein that inhibits viral replication. J. Virol. **72:**1737–1743.
11. **Melegari, M., S. K. Wolf, and R. J. Schneider.** 2005. Hepatitis B virus DNA replication is coordinated by core protein serine phosphorylation and HBx expression. J. Virol. **79:**9810–9820.
12. **Parkin, D. M., P. Pisani, and J. Ferlay.** 1999. Global cancer statistics. CA Cancer J. Clin. **49:**33–64.
13. **Pugh, J. C., K. Yaginuma, K. Koike, and J. Summers.** 1988. Duck hepatitis B virus (DHBV) particles produced by transient expression of DHBV DNA in a human hepatoma cell line are infectious in vitro. J. Virol. **62:**3513–3516.
14. **Rossner, M. T.** 1992. Hepatitis B virus X-gene product: a promiscuous transcriptional activator. J. Med. Virol. **36:**101–117.
15. **Scaglioni, P. P., M. Melegari, and J. R. Wands.** 1997. Posttranscriptional regulation of hepatitis B virus replication by the precore protein. J. Virol. **71:**345–353.
16. **Seifer, M., S. Zhou, and D. N. Standring.** 1993. A micromolar pool of antigenically distinct precursors is required to initiate cooperative assembly of hepatitis B virus capsids in *Xenopus* oocytes. J. Virol. **67:**249–257.
17. **Sitterlin, D., F. Bergametti, P. Tiollais, B. C. Tennant, and C. Transy.** 2000. Correct binding of viral X protein to UVDDB-p127 cellular protein is critical for efficient infection by hepatitis B viruses. Oncogene **19:**4427–4431.
18. **Slagle, B. L., T.-H. Lee, D. Medina, M. J. Finegold, and J. S. Butel.** 1996. Increased sensitivity to the hepatocarcinogen diethylnitrosamine in transgenic mice carrying the hepatitis B virus X gene. Mol. Carcinog. **15:**261–269.
19. **Tang, H., L. Delgermaa, F. J. Huang, N. Oishi, L. Liu, F. He, L. S. Zhao, and S. Murakami.** 2005. The transcriptional transactivation function of HBx protein is important for its augmentation role in hepatitis B virus replication. J. Virol. **79:**5548–5556.
20. **Xu, Z., T. S. B. Yen, L. Wu, C. R. Madden, W. Tan, B. L. Slagle, and J. H. Ou.** 2002. Enhancement of hepatitis B virus replication by its X protein in transgenic mice. J. Virol. **76:**2579–2584.
21. **Yang, P. L., A. Althage, J. Chung, and F. V. Chisari.** 2002. Hydrodynamic injection of viral DNA: a mouse model of acute hepatitis B virus infection. Proc. Natl. Acad. Sci. USA **99:**13825–13830.
22. **Zhang, Z.-S., N. Torii, Z. Hu, J. Jacob, and T. J. Liang.** 2001. X-deficient woodchuck hepatitis virus mutants behave like attenuated viruses and induce protective immunity in vivo. J. Clin. Investig. **108:**1523–1531.
23. **Zoulim, F., J. Saputelli, and C. Seeger.** 1994. Woodchuck hepatitis virus X protein is required for viral infection in vivo. J. Virol. **68:**2026–2030.